Supporting Information

Nanometer-Scale Heterogeneous Interfacial Sapphire Wafer-Bonding for Enabling Plasmonic-Enhanced Nanofluidic Mid-Infrared Spectroscopy

Jikai Xu,[†,‡,¶] Zhihao Ren,[‡,§,¶] Bowei Dong,[‡,§] Xinmiao Liu,[‡,§] Chenxi Wang,[*,†] Yanhong Tian,[*,†] and Chengkuo Lee [*,‡,§,⊥]

[†] *State Key Laboratory of Advanced Welding and Joining, Harbin Institute of Technology, Harbin 150001, China*

[‡] *Department of Electrical and Computer Engineering, National University of Singapore, Singapore 117576, Singapore*

[§] *Center for Intelligent Sensors and MEMS (CISM), National University of Singapore, Singapore 117576, Singapore*

[⊥] *NUS Graduate School for Integrative Sciences & Engineering, National University of Singapore, Singapore 117456, Singapore*

[¶] J.X. and Z.R. contributed equally to this work.

[*] Corresponding authors.

E-mail: *wangchenxi@hit.edu.cn (Chenxi Wang), tianyh@hit.edu.cn (Yanhong Tian), elelc@nus.edu.sg (Chengkuo Lee).*

Contents

Note S1: Simulated electrical field distribution

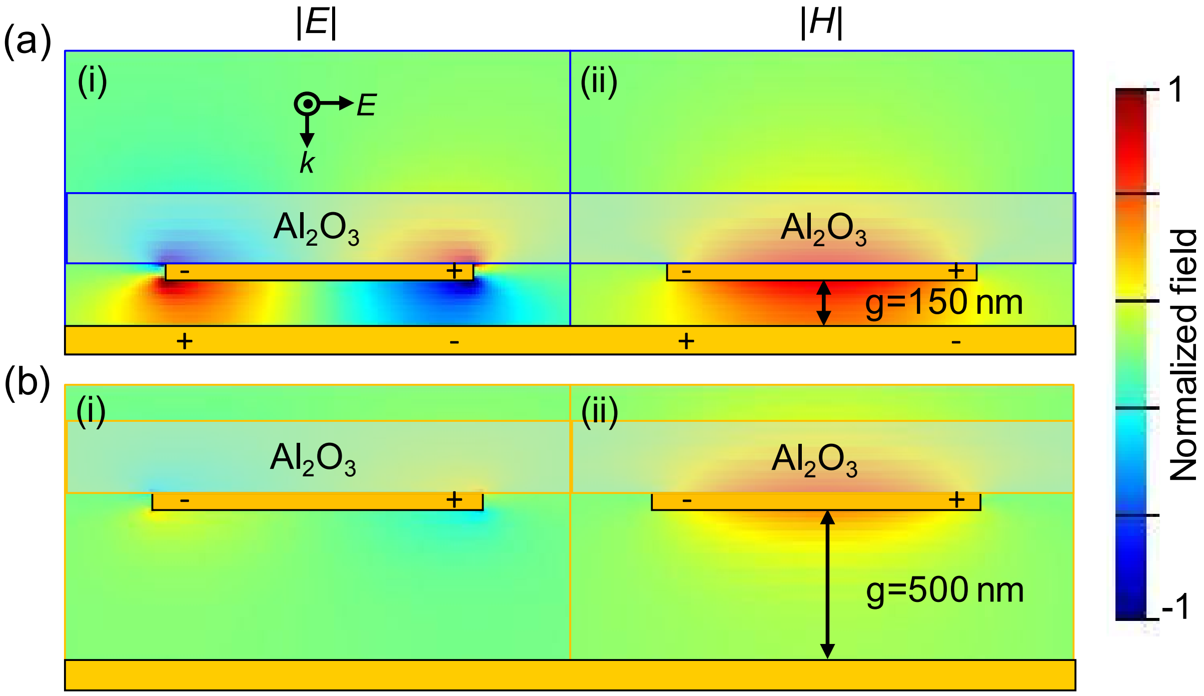

Figure S1. Simulated electrical field distribution along Z direction with Au reflector at different nanogaps: (a) nanogap = 150 nm; (b) nanogap = 500 nm. The quadrupole resonance mode is easily affected by the gap distance. Not only the quadrupole resonance will disappear, but also the resonance intensity will also be weakened when the nanogap is too large.

Note S2: Extraction of external and intrinsic losses

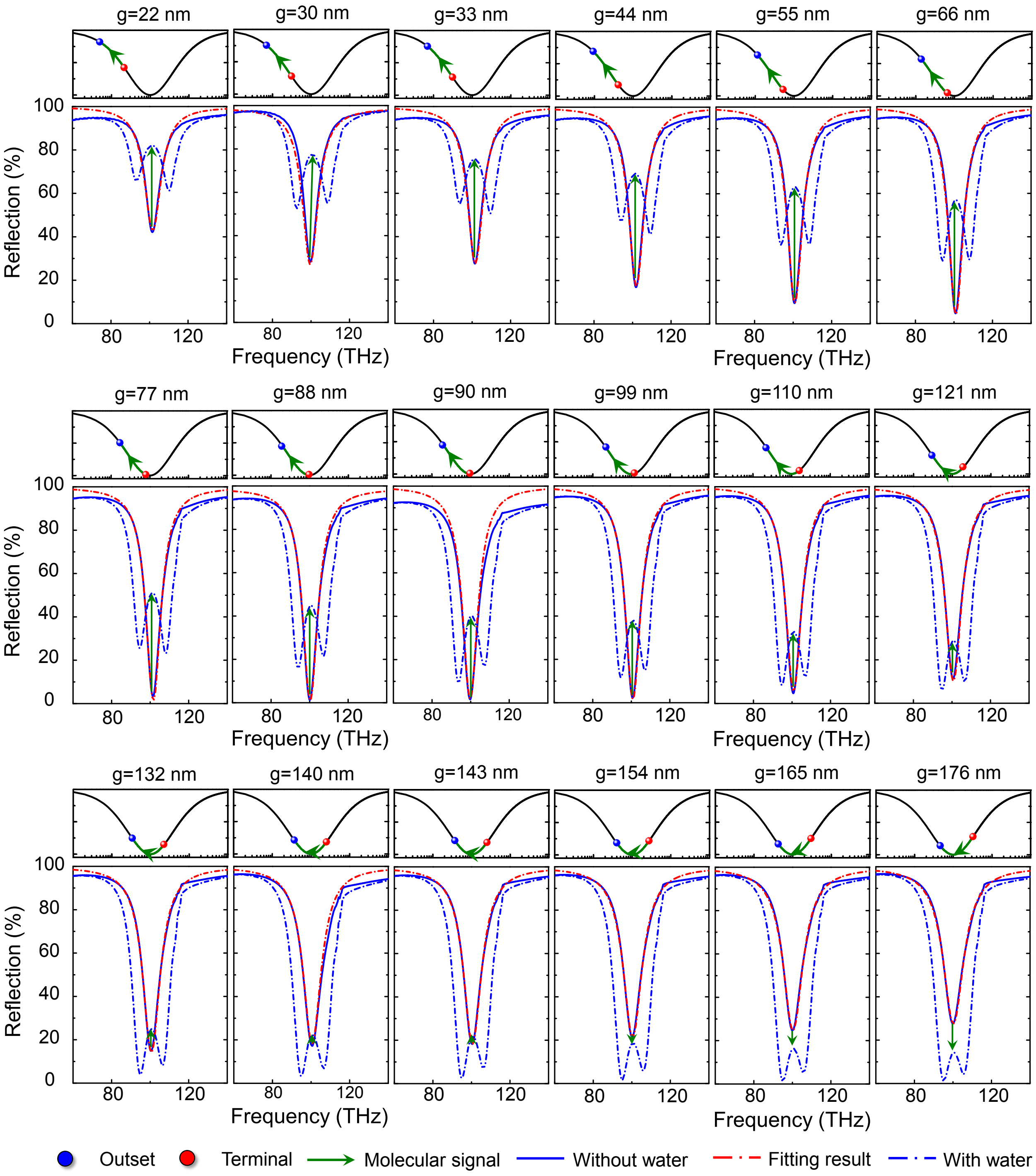

Figure S2. Fitting results of reflection spectra at different nanogaps according to the temporal coupled-mode theory (TCMT).

Table S1. Extraction of external and intrinsic losses at different nanogaps based on TCMT.

Gap	**22**	**30**	**33**	**44**	**55**	**66**	**77**	**88**	**90**
γ_r	0.9013	1.1441	1.1788	1.4180	1.6487	1.8597	2.0815	2.3560	2.3947
γ_a	4.2836	3.9208	3.8018	3.4522	3.1581	2.8315	2.6460	2.4500	2.3024
γ_r/γ_a	0.2104	0.2918	0.3100	0.4108	0.5220	0.6568	0.7867	0.9616	1.0401
R_1	42.45%	29.01%	27.76%	17.27%	9.89%	4.87%	1.50%	1.10%	1.51%
R_2	82.11%	77.25%	75.60%	69.08%	63.11%	56.93%	50.63%	44.73%	43.01%
$\gamma_r/(\gamma_a+\gamma_m)$	0.0494	0.0598	0.0696	0.0926	0.1144	0.1389	0.1688	0.1890	0.1961
Gap	**99**	**110**	**121**	**132**	**140**	**143**	**154**	**165**	**176**
γ_r	2.5979	3.0686	3.3873	3.7650	3.9971	4.0620	4.3813	4.6999	4.9621
γ_a	2.1979	1.9405	1.7951	1.7020	1.6580	1.6273	1.6101	1.5769	1.5431
γ_r/γ_a	1.1820	1.5813	1.8870	2.2121	2.4108	2.4962	2.7211	2.9805	3.2158
R_1	1.90%	5.08%	10.79%	15.04%	17.65%	18.48%	21.82%	24.93%	28.04%
R_2	37.81%	32.88%	28.70%	24.66%	21.97%	21.50%	18.63%	16.30%	13.98%
$\gamma_r/(\gamma_a+\gamma_m)$	0.2180	0.2640	0.2980	0.3376	0.3483	0.3689	0.3984	0.4254	0.4576

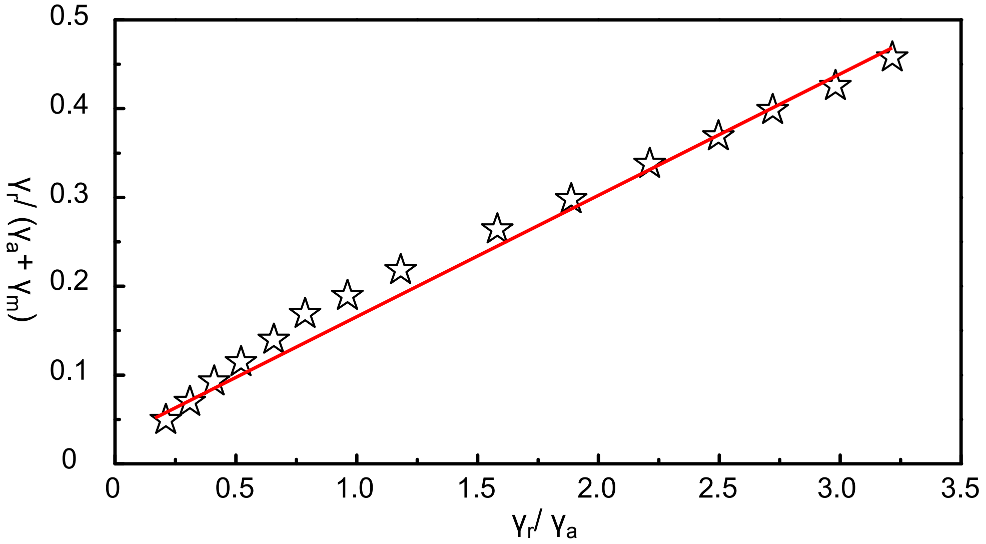

Figure S3. Relationship between γ_r/γ_a and $\gamma_r/(\gamma_a + \gamma_m)$ according to the extracted data.

Note S3: Theoretical calculation of the signal enhancement

In section S3, we demonstrate the theoretical calculation of the signal enhancement based on the temporal coupled-mode theory (TCMT). We can derive the signal enhancement by the difference between the spectra with and without the analyte absorption. Detailed theoretical calculations are as follows:

(1) Without analyte absorption:

General equations of the TCMT can be described as follows:

$$\frac{d\mathrm{P}}{dt} = jw_0 P - (\gamma_a + \gamma_r)P + ks_+ \tag{S1}$$

$$s_- = -s_+ + k\mathrm{M} \tag{S2}$$

where P is the mode amplitude of the plasmonic structure. ω_0 is the resonance frequency of the plasmonic structure. We can obtain the following formulas by calculating (S1) and (S2):

$$jwA = jw_0 A - (\gamma_a + \gamma_r)A + ks_+ \tag{S3}$$

$$s_+ = \frac{j(w - w_0) + (\gamma_a + \gamma_r)}{k}A \tag{S4}$$

$$s_- = \frac{k^2 - j(w - w_0) - (\gamma_a + \gamma_r)}{k}A \tag{S5}$$

Therefore, the calculated results of the reflection spectra from (S1) and (S2) are as follows:

$$R = \left|\frac{s_-}{s_+}\right|^2 = \left|\frac{k^2 - j(w - w_0) - (\gamma_a + \gamma_r)}{j(w - w_0) + (\gamma_a + \gamma_r)}\right|^2 \tag{S6}$$

Due to the plasmonic nanofluidic is single port resonance system, so:

$$k = \sqrt{2\gamma_{\mathrm{r}}}$$

Changes in reflection spectra with frequency (w) can be expressed as follows:

$$R = \left|\frac{s_-}{s_+}\right|^2 = \left|\frac{j(w - w_0) - (\gamma_r - \gamma_a)}{j(w - w_0) + (\gamma_a + \gamma_r)}\right|^2 \tag{S7}$$

The reflection dip can be obtained when $w = w_0$:

$$R = \left|\frac{\gamma_\mathrm{r} - \gamma_a}{\gamma_a + \gamma_r}\right|^2 \tag{S8}$$

(2) With analyte absorption:

By adding the analyte absorption, the derivations are as follows:

$$\frac{dP}{dt} = jw_0P - (\gamma_a + \gamma_r)A + j\mu M + ks_+ \tag{S9}$$

$$\frac{dM}{dt} = jw_mM - \gamma_mM + j\mu P \tag{S10}$$

$$s_- = -s_+ + kA \tag{S11}$$

$$R = \left|\frac{s_-}{s_+}\right|^2 \tag{S12}$$

$$s_+ = \frac{j(w - w_0) + (\gamma_a + \gamma_r) + \dfrac{\mu^2}{j(w - w_m) + \gamma_m}}{k}P \tag{S13}$$

$$s_- = \frac{k^2 - j(w - w_0) - (\gamma_a + \gamma_r) - \dfrac{\mu^2}{j(w - w_m) + \gamma_m}}{k}P \tag{S14}$$

$$R_A = \left|\frac{s_-}{s_+}\right|^2 = \left|\frac{k^2 - j(w - w_0) - (\gamma_a + \gamma_r) - \dfrac{\mu^2}{j(w - w_m) + \gamma_m}}{j(w - w_0) + (\gamma_a + \gamma_r) + \dfrac{\mu^2}{j(w - w_m) + \gamma_m}}\right|^2 \tag{S15}$$

where μ is the coupling strength. M is the molecular vibration. ω_m is the resonance frequency of the molecular vibration. When $w = w_0$,

$$R_A = \left|\frac{(\gamma_r - \gamma_a) - \dfrac{\mu^2}{j(w - w_m) + \gamma_m}}{(\gamma_a + \gamma_r) + \dfrac{\mu^2}{j(w - w_m) + \gamma_m}}\right|^2 = \left|\frac{\gamma_r - \left(\gamma_a + \dfrac{\mu^2}{j(w - w_m) + \gamma_m}\right)}{\gamma_r + \left(\gamma_a + \dfrac{\mu^2}{j(w - w_m) + \gamma_m}\right)}\right|^2 \quad \text{(S16)}$$

We assume that:

$$\gamma_\mu = \frac{\mu^2}{j(w - w_m) + \gamma_m} \quad \text{(S17)}$$

$$\gamma_a' \rightarrow \gamma_a + \gamma_m \quad \text{(S18)}$$

Therefore, we can get the reflection by submitting (S17) and (S18) into (S16):

$$R_A = \left|\frac{\gamma_r - \gamma_a'}{\gamma_r + \gamma_a'}\right|^2 \quad \text{(S19)}$$

(3) Enhanced signal:

The enhanced signal is the difference between the coupling with and without analyte absorptions at the resonance frequency:

$$\Delta R_A = R_{H_2O} - R = \left|\frac{\gamma_r - \gamma_a'}{\gamma_r + \gamma_a'}\right|^2 - \left|\frac{\gamma_r - \gamma_a}{\gamma_r + \gamma_a}\right|^2 \quad \text{(S20)}$$

We assume that:

$$f = \frac{\gamma_r}{\gamma_a} \quad \text{(S21)}$$

$$f' = \frac{\gamma_r'}{\gamma_a} \quad \text{(S22)}$$

Then we can get the enhanced signal:

$$\Delta R_A = \left|\frac{f' - 1}{f' + 1}\right|^2 - \left|\frac{f - 1}{f + 1}\right|^2 = 4\frac{(f'f - 1)(f' - f)}{(f' + 1)^2(f + 1)^2} \tag{S23}$$

According to the result fitting result that f' is approximately positively correlated to f:

$$f' \backcong tf \tag{S24}$$

Therefore, the enhanced signal can be obtained:

$$\Delta R_A \propto \frac{(tf^2 - 1)(t - 1)f}{(tf + 1)^2(f + 1)} \tag{S25}$$

Note S4: Bonding strength measurement

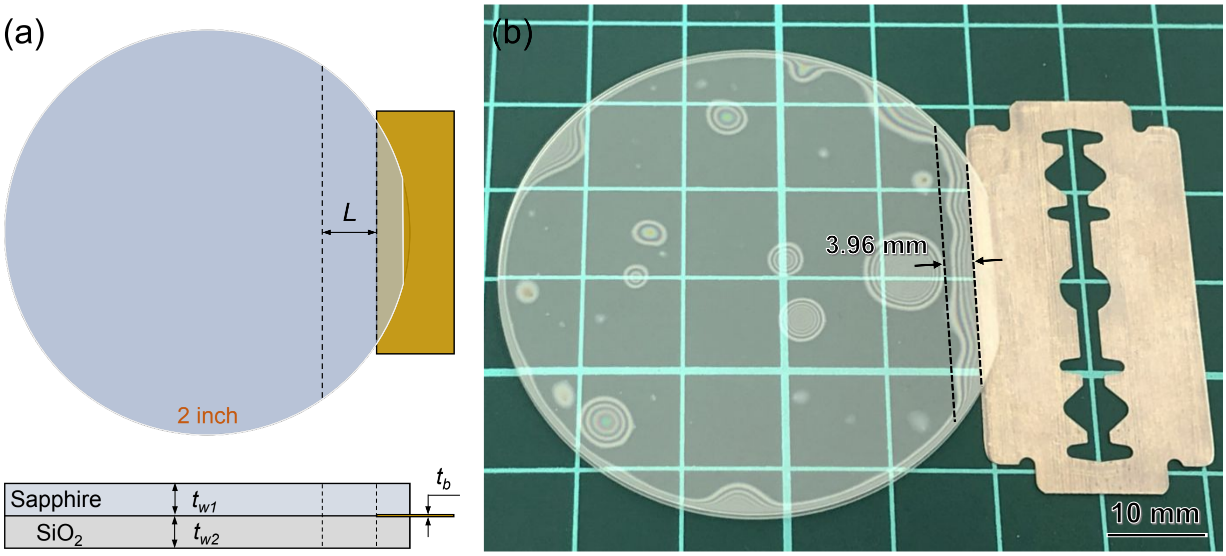

Figure S4. Measurement for the Al_2O_3/SiO_2 bonding energy. (a) The schematic diagram for the bonding strength calculation. (b) Optical image of the bonded Al_2O_3/SiO_2 wafer with the blade insertion.

Note S5: Surface characterization of SiO_2 and Al_2O_3 surfaces by XPS

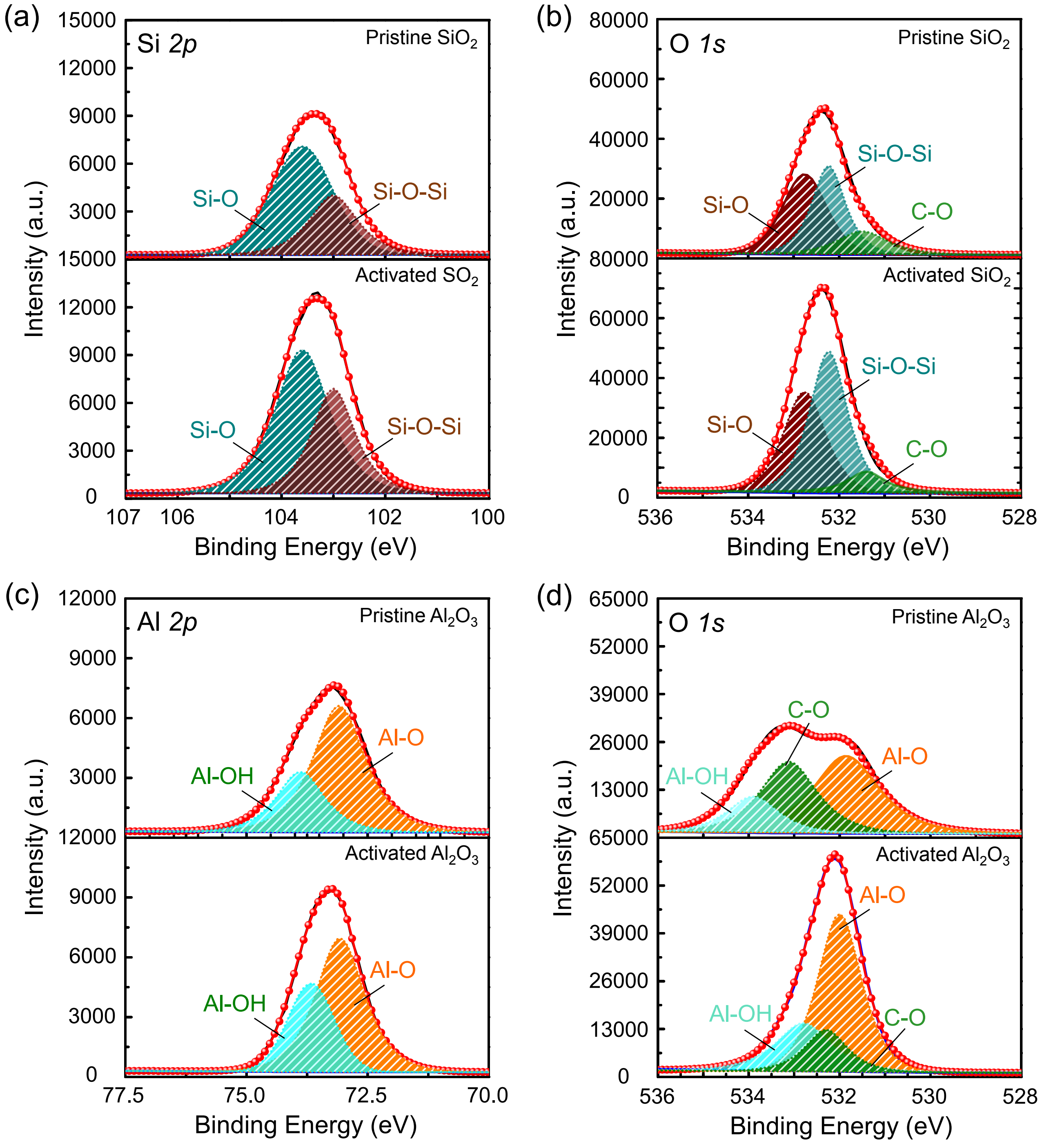

Figure S5. Surface characterization by XPS: (a, b) Si *2p* and O *1s* core spectra for SiO_2 substrates before and after the plasma activation. (c, d) Al *2p* and O *1s* core spectra for Al_2O_3 substrates before and after the plasma activation.

Note S6: Spectra tuning and enhanced H_2O signal detection

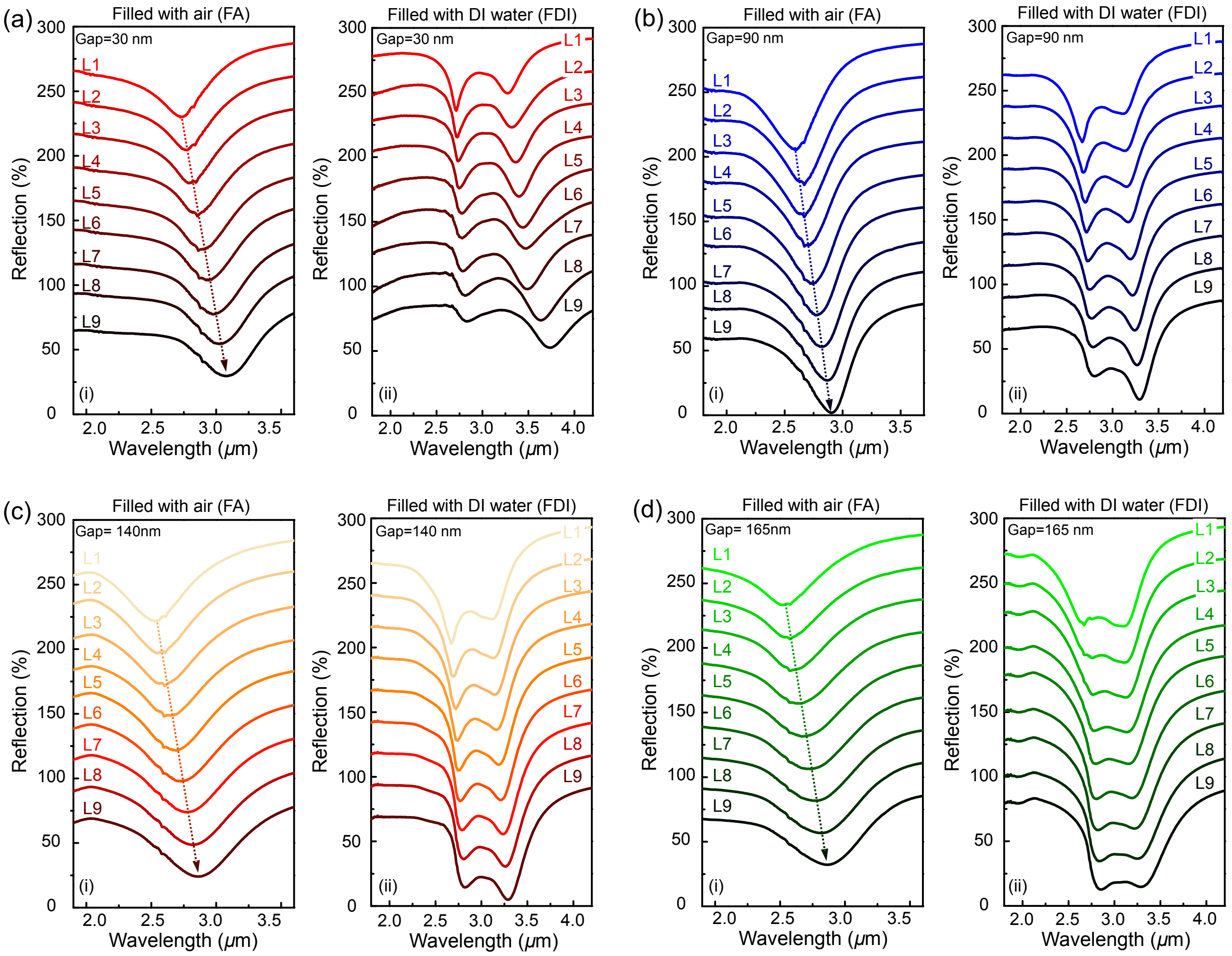

Figure S6. Spectra tuning and enhanced H_2O signal detection at different nanogaps: Measured reflection spectra of the plasmonics-nanofluidics filled with air and DI water at the gap of (a) 30 nm, (b) 90 nm, (c) 140 nm, and (d) 165 nm. To tune the resonance spectra, the nanoantenna length is varied from 572 nm to 668 nm with an interval of 12 nm.

Note S7: Measurement for nanogaps

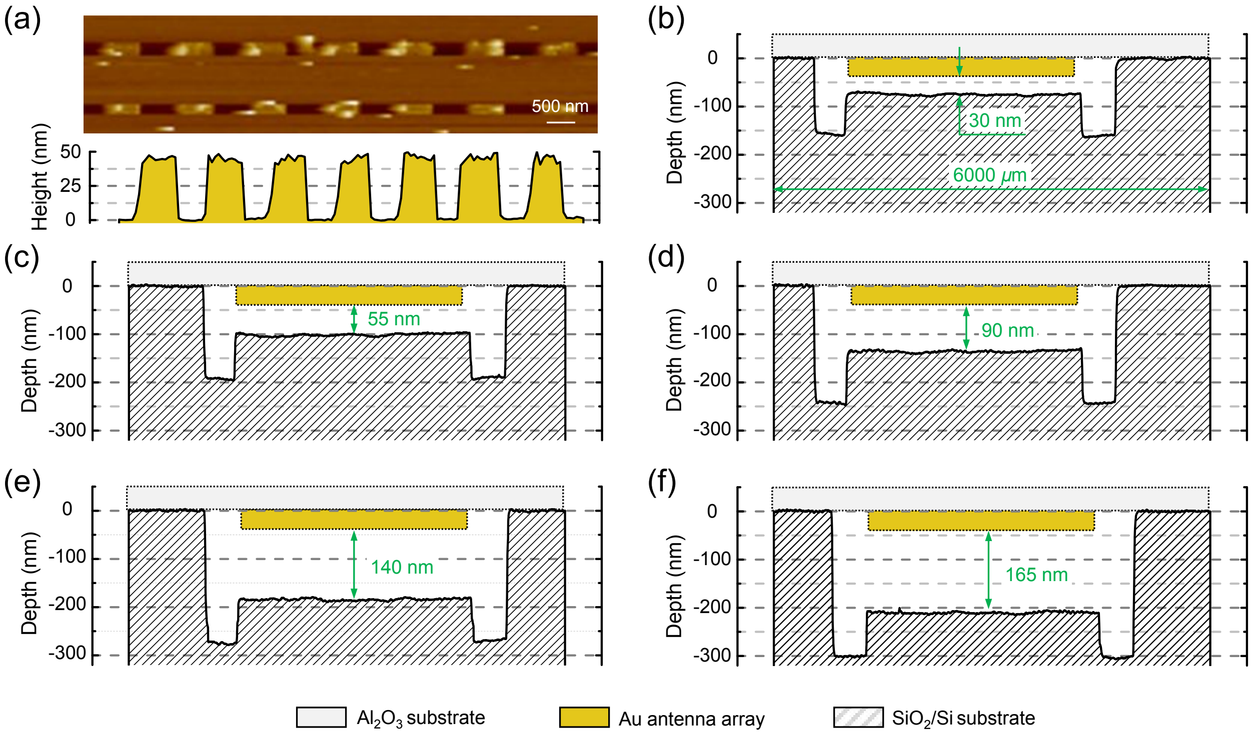

Figure S7. Measurement for nanogaps. (a) AFM image for Au antennas fabricated on the Al_2O_3 substrate. The curve below the AFM image shows the antenna profiles along the height direction. The antenna heights are around 45 nm. (b)-(f) Etching profiles of SiO_2 substrates for 30 nm, 55 nm, 90 nm, 140 nm, and 165 nm-nanogap plasmonic nanofluidics.

Note S8: Device fabrication process

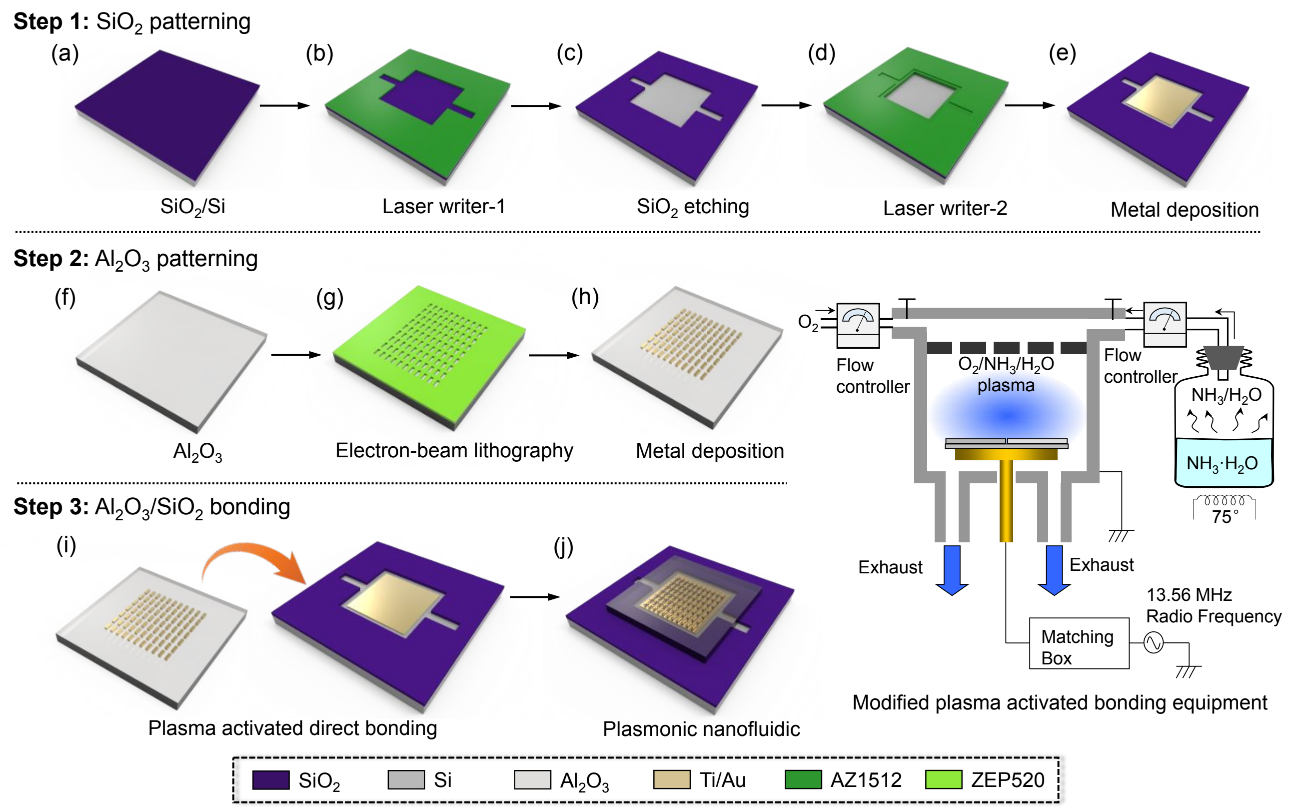

Figure S8. The fabrication process of plasmonics-nanofluidics device: (a-e) fabrication of the sensing chamber with Au reflector. To avoid the deposited Au film will cause the protrusion of the edges and induce the bonding failure, we repeat the laser writer and SiO$_2$ etching processes twice to avoid the contact between the deposited Au film and edges. (f-h) nanoantenna fabrication on Al$_2$O$_3$ substrate by electron beam lithography and electron beam evaporator. (i-j) plasma-activated direct bonding of Al$_2$O$_3$ and SiO$_2$ to integrate the plasmonics-nanofluidic device. The insert in the right corner is the modified plasma-activated direct bonding equipment.

Note S9: Calculation for the number of acetone molecules

According to the simulations of the electric field distribution shown in Figure 1e, the sensing area is mainly concentrated in the space sandwiched by the nanoantennas and Au reflector. The schematic diagram of the plasmonic nanofluidic is shown in Figure S8.

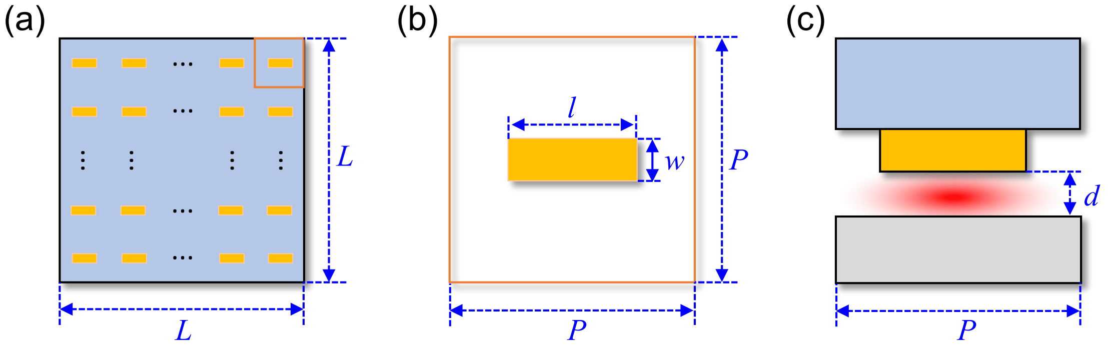

Figure S9. Schematic diagram of the plasmonic nanofluidic. (a) Au nanoantenna array fabricated on the sapphire substrate. The length (*L*) of the Au nanoantenna array is 200 μm. (b) One unit of the Au nanoantenna array. The period (*P*) is 1.5μm. The length (*l*) and width (*w*) of the Au nanoantenna are 608 nm and 200 nm, respectively. (c) Cross-section of the plasmonic nanofluidic. The nanogap (*d*) between the Au nanoantenna and SiO_2 substrate is 55 nm.

Therefore, the total sensing volume can be expressed as follows:

$$V_T = L^2 \cdot \frac{l \cdot w}{P^2} \cdot d, \tag{S26}$$

where V_T is the total sensing volume, L is the length of the Au nanoantenna array, l is the nanoantenna length, w is the nanoantenna width, P is the period of the nanoantenna array, and d is nanogap between the nanoantenna and SiO_2 substrate.

So the number of acetone molecules can be obtained as follows:

$$N = \frac{V_T \cdot C_A}{V_A}, \tag{S27}$$

where C_A and V_A are the concentration and molar volume of acetone, respectively. The V_A is

75.1×10^{-9} m^3/mol.

By submitting (S26) into (S27), the final equation for the number of acetone molecules is obtained as follows:

$$N = L^2 \cdot \frac{l \cdot w}{P^2} \cdot d \cdot \frac{C_A}{75.1 \times 10^{-9}}. \tag{S28}$$

Note S10: Dynamic monitoring for ethanol diffusion

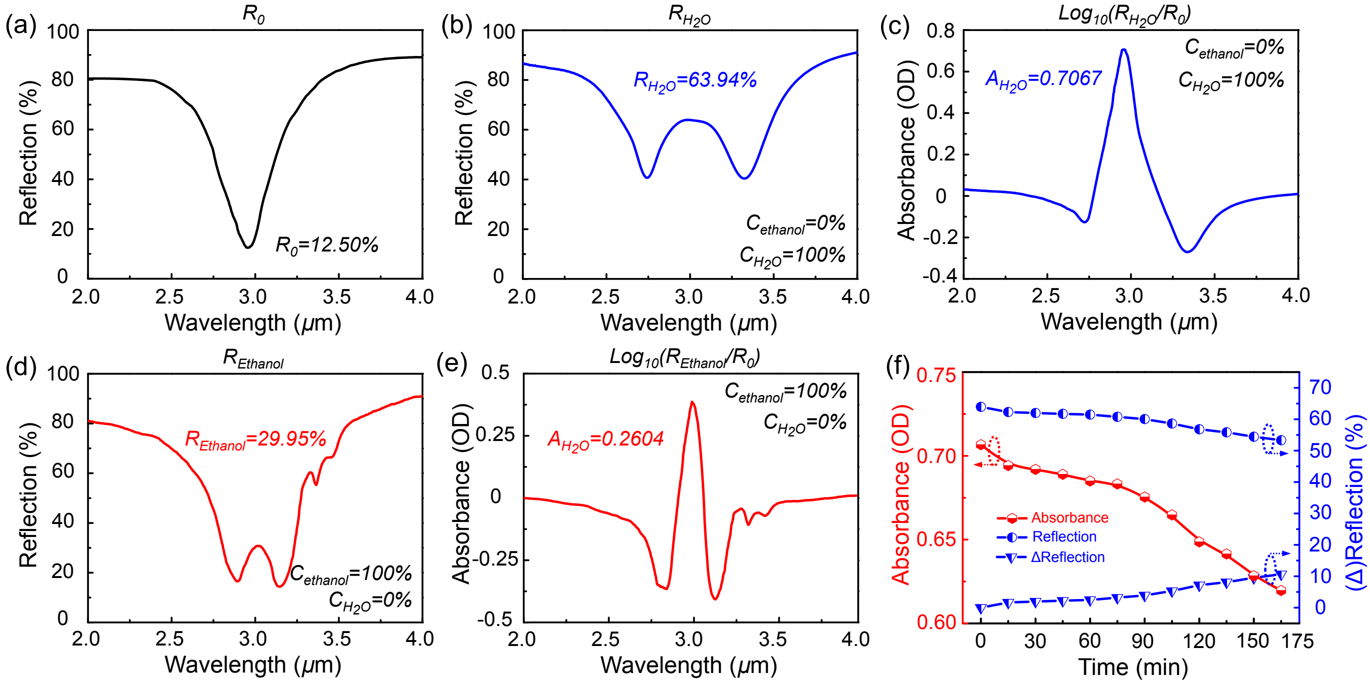

Figure S10. Dynamic monitoring for ethanol diffusion. Measured reflection spectra when the plasmonic-enhanced nanofluidic filled with (a) acetone, (b) DI water, and (d) ethanol. Differential absorption spectra for DI water and ethanol are shown in (c) and (e), respectively. (f) Statistical results of absorbance, reflection dips, and reflection differences at different times.